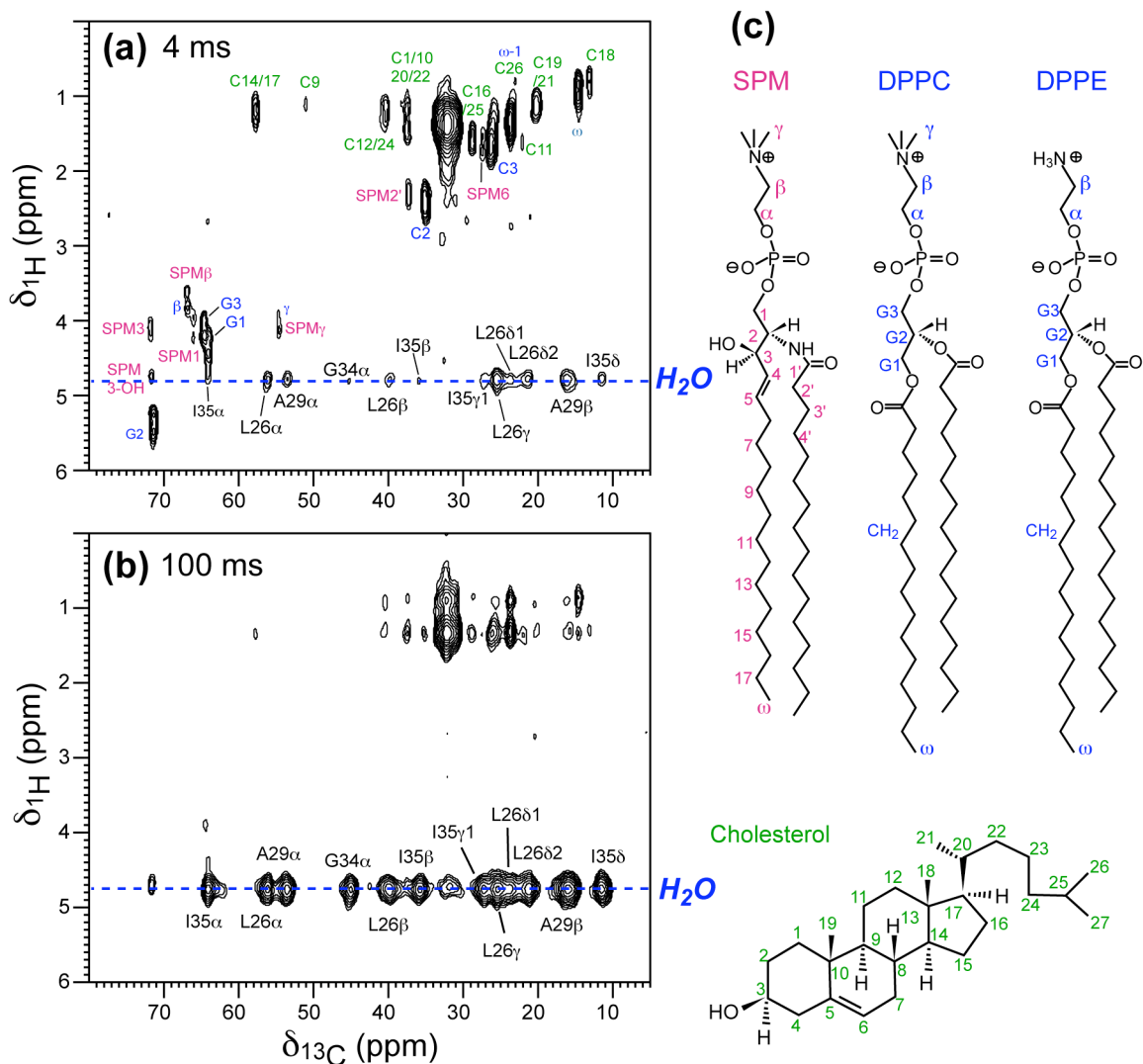


## **Supplementary Information**

### **Conformational Changes of an Ion Channel Detected Through Water-Protein Interactions Using Solid-State NMR Spectroscopy**

Wenbin Luo and Mei Hong

Department of Chemistry, Iowa State University, Ames, IA 50011



**Fig. S1.** Representative full 2D  $^{13}\text{C}$ - $^1\text{H}$  spin diffusion correlation spectra of M2-TM in viral membranes. The sample is the amantadine-bound M2-TM at pH 7.5. The spectra were measured at 293 K under 5 kHz MAS using a  $^1\text{H}$   $T_2$  filter of 2 ms and varying spin diffusion mixing times. (a) 4 ms mixing. (b) 100 ms mixing. Intermolecular water-protein cross peaks are assigned in black. Intramolecular lipid and cholesterol  $^1\text{H}$ - $^{13}\text{C}$  cross peaks are also assigned. Cholesterol: green. Phospholipids: blue. Sphingomyelin (SPM): magenta.

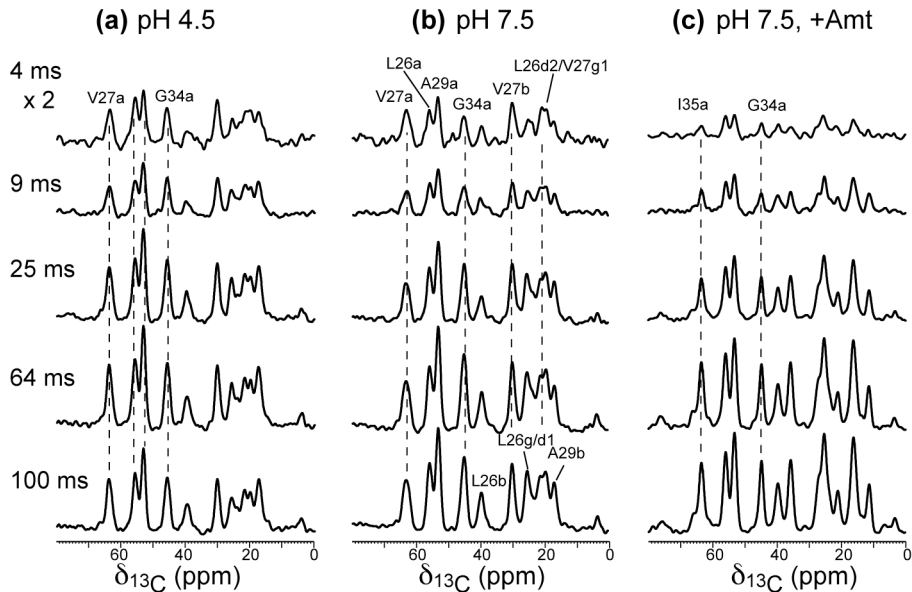


**Fig. S2.**  $^{13}\text{C}$  DQ filtered spectra of M2-TM in viral membranes after  $^1\text{H}$  spin diffusion from water. All spectra were measured using a  $^1\text{H}$   $T_2$  filter of 2 ms at 293 K under 5 kHz MAS. Spin diffusion mixing times are indicated on the left. (a) pH 4.5. (b) pH 7.5. (c) pH 7.5 with amantadine. The spectra were plotted to scale within each sample.  $^1\text{H}$  spin diffusion from water to Gly<sub>34</sub> is slower than to N-terminal residues in the amantadine-bound sample, but is comparable in the two apo samples. Thus, in the absence of drug, both the low and high pH pores contain significant amount of water, while amantadine interrupts the water pathway between Ala<sub>29</sub> and Gly<sub>34</sub>. In the two apo samples, water-Ala<sub>29</sub> spin diffusion is slightly slower than water-Val<sub>27</sub> and water-Leu<sub>26</sub> spin diffusion, consistent with the lipid-facing position of Ala<sub>29</sub>.

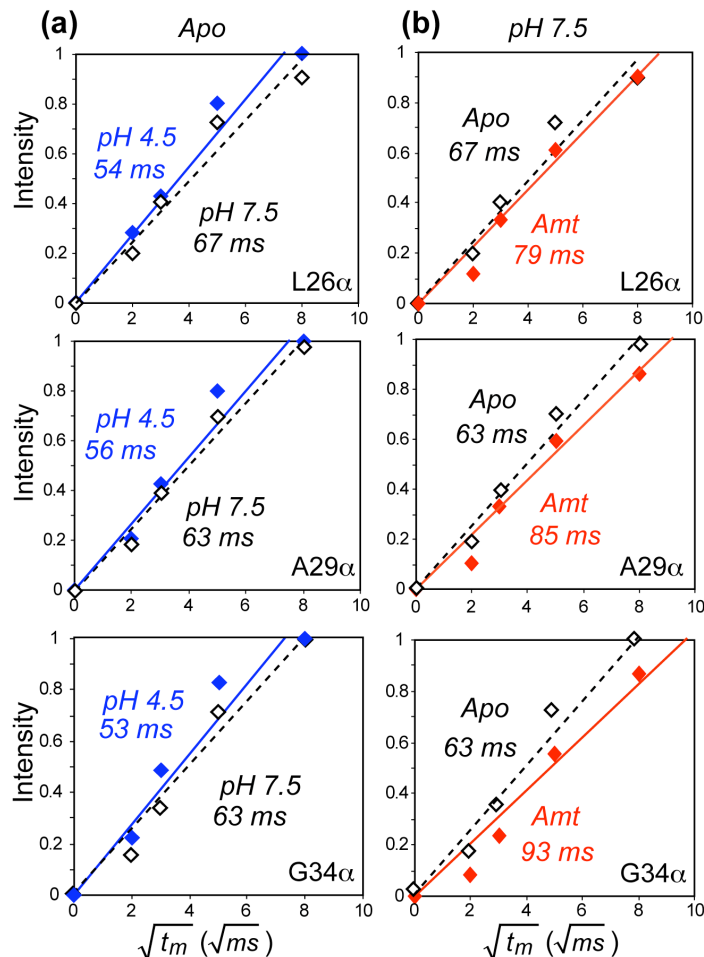


**Fig. S3.** Linear fitting of the initial rates of the water-to-M2  $^1\text{H}$  spin diffusion buildup curves to extract  $t_m^S$  values. Intensities are obtained from the 1D  $^{13}\text{C}$  DQ filtered spectra (Fig. S2). (a) Comparison of the pH 4.5 (blue) and pH 7.5 (black) data without amantadine. (b) Comparison of the apo pH 7.5 data (black) and the amantadine-bound pH 7.5 data (red). For all labeled sites, the amantadine-bound protein at pH 7.5 has the longest  $t_m^S$  values, indicating that it has the lowest water accessibility, while the apo M2 at pH 4.5 has the shortest  $t_m^S$  values, indicating that the open state has the highest water accessibility.

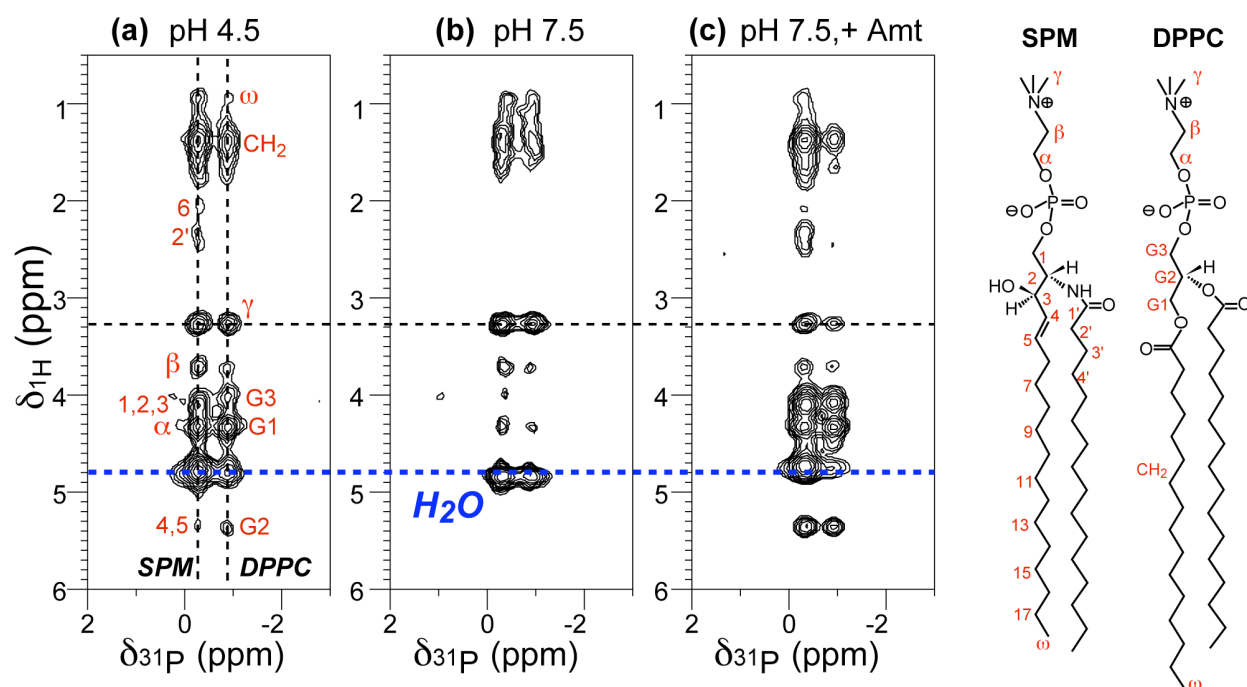


**Fig. S4.** 2D  $^1\text{H}$ - $^{31}\text{P}$  correlation spectra of membrane-bound M2-TM after  $^1\text{H}$  spin diffusion. The spectra were measured with a  $^1\text{H}$   $T_2$  filter of 0.8 ms and a spin diffusion mixing time of 64 ms at 293 K under 7 kHz MAS. (a) pH 4.5. (b) pH 7.5. (c) pH 7.5 with amantadine. Peak assignment is given in (a) along with the chemical structure and nomenclature of sphingomyelin (SPM) and DPPC on the right. The lipid  $\text{H}_\gamma$  signal is calibrated to be 3.26 ppm in each spectrum.

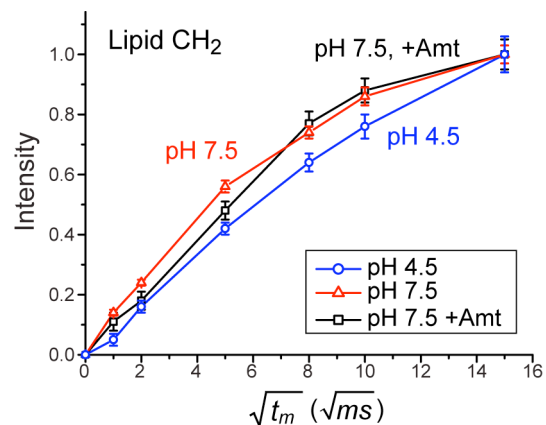


**Fig. S5.** Water-to-lipid spin diffusion for M2-containing viral membranes. Single-quantum  $^{13}\text{C}$  spectra were measured with a  $^1\text{H}$   $T_2$  filter time of 2.2 ms and varying spin diffusion mixing times at 293 K under 5 kHz MAS. The complete suppression of the initial lipid  $^1\text{H}$  magnetization by the  $T_2$  filter was confirmed by null intensity of the lipid  $\text{CH}_2$  peak when the mixing time was set to 0. The low-pH membrane shows the slowest water-lipid spin diffusion, while the two high-pH samples have similar buildup rates with or without amantadine. This trend is different from and partly opposite to the water-protein spin diffusion behavior, indicating that the water-protein spin diffusion changes uniquely result from water accessibility changes of the protein, not from diffusion rate changes of water or lipids.

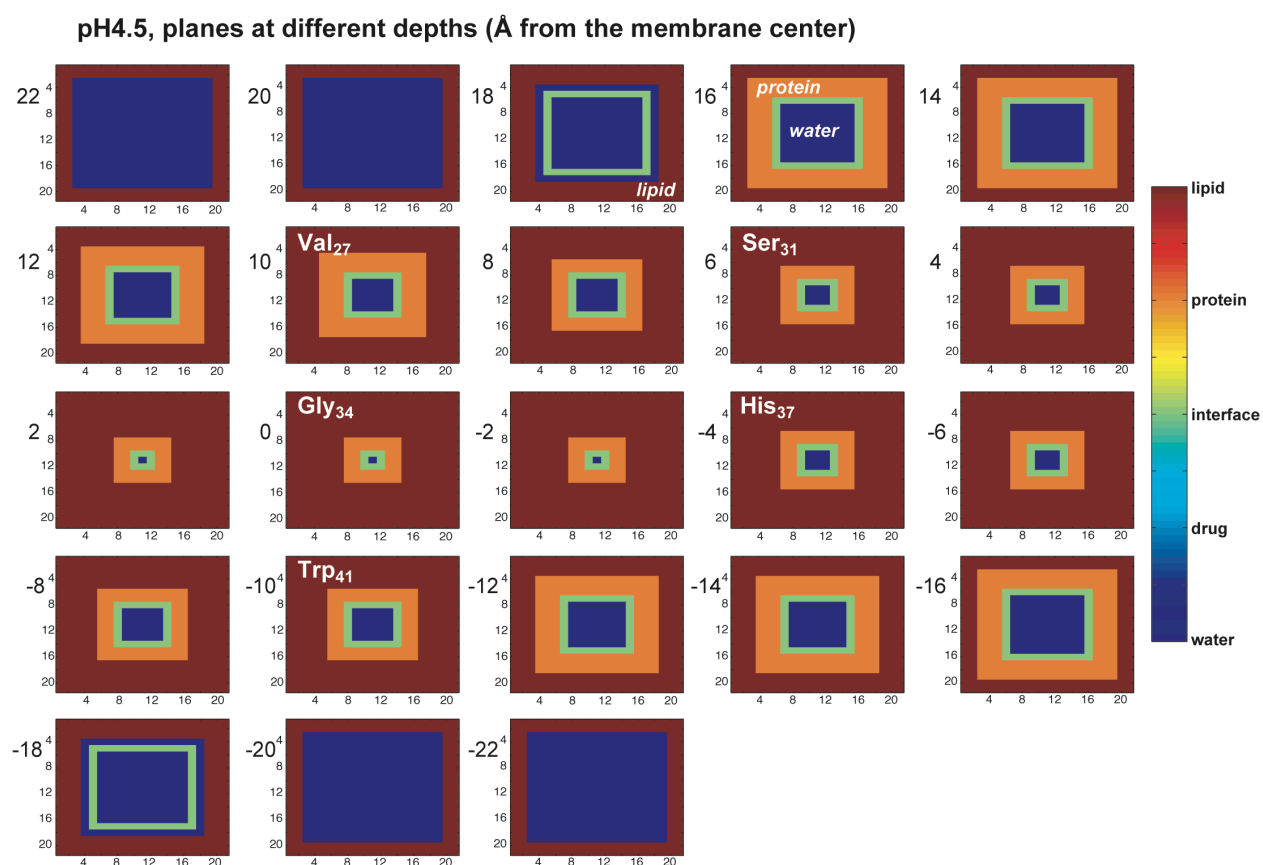


**Fig. S6.** Three-dimensional lattice used in the best-fit simulation of the water-to-protein spin diffusion buildup curve of M2-TM at pH 4.5. The spatial distributions of the water (dark blue), protein (orange), water-protein interface (green), and lipid (brown) cubes are shown for 23 planes spaced at 2  $\text{\AA}$  intervals along the bilayer normal. Approximate z-positions of key pore-lining residues on the lattice are indicated at appropriate planes.

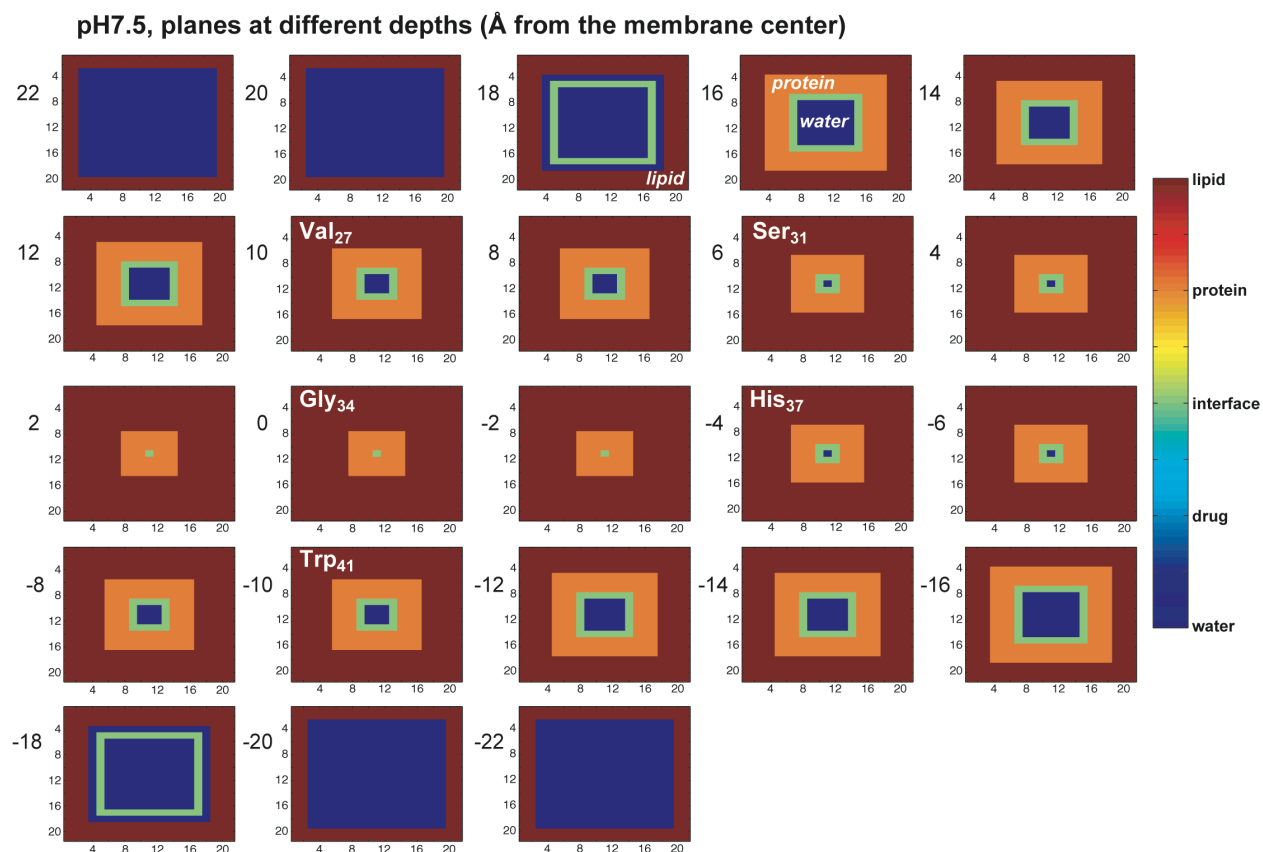


**Fig. S7.** Three-dimensional lattice used in the best-fit simulation of the water-to-protein spin diffusion buildup curve of M2-TM at pH 7.5 without amantadine. The spatial distributions of the water (dark blue), protein (orange), water-protein interface (green), and lipid (brown) cubes are shown for 23 planes spaced at  $2 \text{ \AA}$  intervals along the bilayer normal. Approximate z-positions of key pore-lining residues on the lattice are indicated.



pH 7.5 + Amt, planes at different depths (Å from the membrane center)

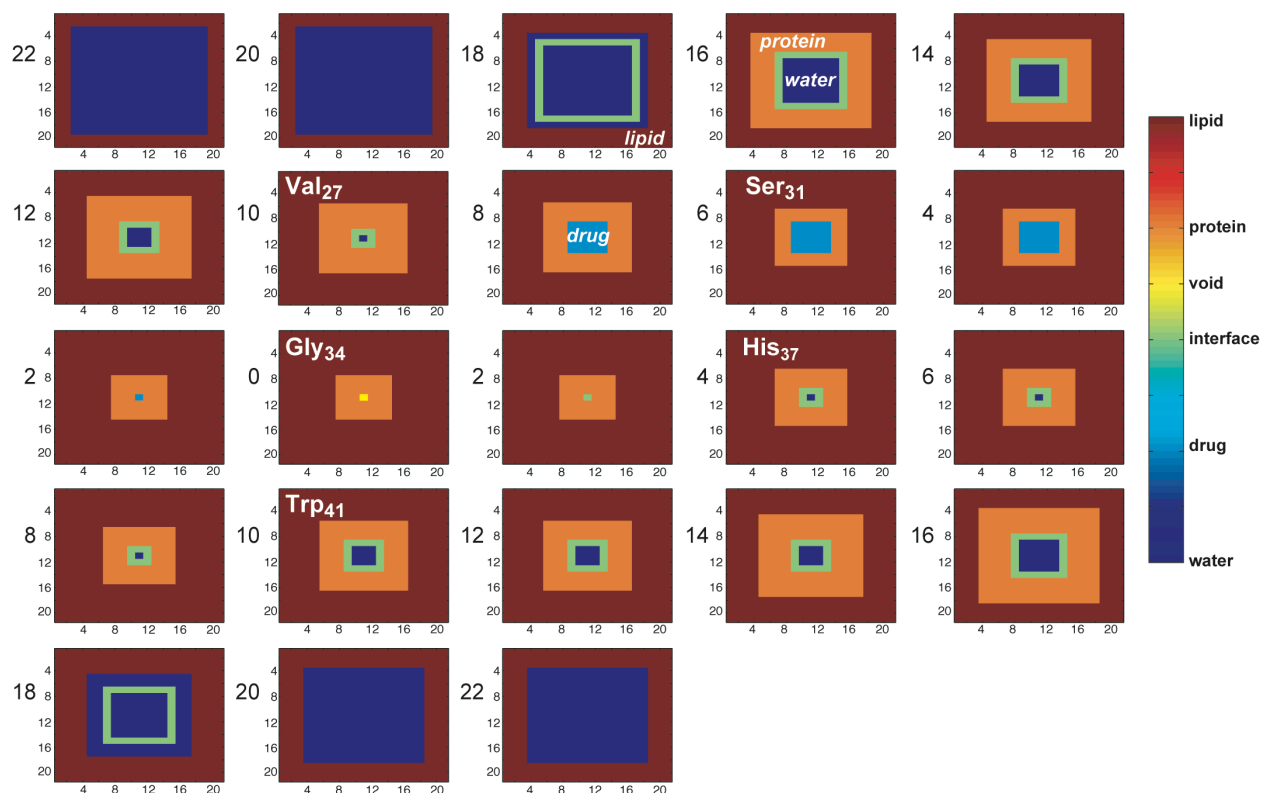


**Fig. S8.** Three-dimensional lattice used in the best-fit simulation of the water-to-protein spin diffusion buildup curve of amantadine-bound M2-TM at pH 7.5. The spatial distributions of water (dark blue), protein (orange), water-protein interface (green), amantadine (cyan), and lipid (brown) cubes are shown for 23 planes spaced at 2 Å intervals along the bilayer normal. Approximate z-positions of key pore-lining residues on the lattice are indicated. Note the exact z-position of the drug is qualitative and is not precisely determined from the current experiments.

**Table S1.**  $t_m^S$  values (ms) from the initial buildup rates of the  $^{13}\text{C}$  DQ filtered  $^1\text{H}$  spin diffusion spectra of M2-TM under different conditions.

Site	pH 4.5	pH 7.5	pH 7.5 + Amt
L26 $\alpha$	54 $\pm$ 5	67 $\pm$ 7	79 $\pm$ 8
L26 $\beta$	57 $\pm$ 4	69 $\pm$ 8	83 $\pm$ 8
L26 $\gamma$	53 $\pm$ 7	68 $\pm$ 8	82 $\pm$ 9
L26 $\delta$ 1	55 $\pm$ 6	68 $\pm$ 8	85 $\pm$ 9
L26 $\delta$ 2/V27 $\gamma$ 1	56 $\pm$ 5	66 $\pm$ 5	-
V27 $\alpha$	59 $\pm$ 6	66 $\pm$ 6	-
V27 $\beta$	57 $\pm$ 6	56 $\pm$ 6	-
V27 $\gamma$ 2	52 $\pm$ 6	57 $\pm$ 5	-
A29 $\alpha$	56 $\pm$ 6	63 $\pm$ 5	85 $\pm$ 9
A29 $\beta$	55 $\pm$ 6	68 $\pm$ 10	84 $\pm$ 10
G34 $\alpha$	53 $\pm$ 7	63 $\pm$ 6	93 $\pm$ 12
I35 $\alpha$	-	-	87 $\pm$ 11
I35 $\beta$	-	-	91 $\pm$ 13
I35 $\delta$	-	-	88 $\pm$ 11
Mean	55 $\pm$ 6	66 $\pm$ 7	86 $\pm$ 10